Union of the discretized spectra for multichannel resonances

V. N. Pomerantsev,* O. A. Rubtsova,† and V. A. Kulikov‡
Skobeltsyn Institute of Nuclear Physics, Moscow State University, 119991 Moscow, Russia

(Received 17 July 2023; accepted 9 December 2023; published 19 January 2024)

Background: Resonances with binary and few-body decay modes, such as the excited and ground states of neutron- and proton-rich nuclei, are important objects in nuclear physics. However, a description of three- and few-body states in the continuum and their decays, especially in case of the Coulomb interaction, remains a hardly solvable problem.
Purpose: We aim to develop an effective technique for finding the parameters of multichannel resonances based on the analysis of discretized spectra without explicitly taking into account boundary conditions.
Methods: We introduce a new method for analyzing discretized spectra using spectral and integrated densities of states. For multichannel two-body scattering problems, this approach allows to one calculate a sum of the eigen phase shifts as well as the resonance parameters via solving an eigenvalue problem for the total and asymptotic Hamiltonian matrices in some L^2 basis. The generalization of the method to the three-body continuum is used to find the positions and widths of the resonances.
Results: We test the presented approach for several multichannel problems and for the three-particle αNN model for light nuclei with $A = 6$. In particular, the width of the ^{6}Be ground state and the parameters of the 3^+0 resonance for the ^{6}Li nucleus are found from a diagonalization of the matrix Hamiltonian with realistic interactions on the Gaussian basis.
Conclusions: The proposed method can be employed to study three-body decays in nonbinary channels, such as the decay that accompanies two-proton radioactivity.

DOI: 10.1103/PhysRevC.109.014002

I. INTRODUCTION

Resonances are basic objects of nuclear physics, representing the excited and ground states of rare isotopes, neutron- or proton-rich nuclei, and weakly bound nuclei. One of the most challenging and relevant problems here is the description of two-proton radioactivity [1,2]. Unlike true bound states, resonances belong to the continuum and their consideration requires taking into account various asymptotic channels and corresponding boundary conditions. The most strict way to find resonance parameters is a calculation of the S matrix and its analytical continuation into the complex energy plane [3,4]. However, to date, an accurate description of three- and few-particle systems, especially in the case of charged particles, remains a hardly solvable problem.

To simplify practical calculations, the idea of solving problems in continuum via its discretization is fruitful [5–17]. The main goal of methods based on the L^2 discretization for a few-body continuum is to reduce the complexity of the problem to the level of the bound-state problem [17]. Such a reduction seems to be realizable, at least for the problem of finding resonance parameters.

There are many L^2-type methods which have been elaborated for solving problems in the continuum and can be employed to find resonance parameters. Here we should mention the R-matrix [5] and J-matrix [6] approaches, the finite volume approach [7,8], calculations in the analytical basis of the transformed harmonic oscillator [9], complex scaling [10–13], the Gamow coupled-channels method using complex momenta [14], and many other methods. The complex scaling approach seems to be the closest to the desired way to solve the problem, since it allows one to find the positions of the resonances just from the spectrum of the Hamiltonian matrix. However, this approach requires a transformation of variables into the complex plane, has several restrictions on interactions, and becomes more complex for a few-body system. Only a few of the L^2 approaches are used for realistic calculations of three-body and few-body resonances (see, for example, [6,8,9,11,13,14]).

In this paper, we propose a new technique for analyzing a discretized continuum based on the spectral shift function and the spectral density formalism [18–20]. The spectral shift function (SSF) [21,22] and spectral densities [11,23] are known in scattering theory due to the trace formula and spectral integrals, such as the virial expansion [23]. At the same time, these objects are directly related to the S matrix and, therefore, can be used both to solve a scattering problem and to search for resonance parameters. We recently showed [19] that the SSF formalism is very well suited for the L^2 discretization approaches. In particular, the phase shift of one-channel scattering in the two-body problem can be found from the difference between the integrated spectral densities (ISDs) for the total and asymptotic Hamiltonians. To find these ISDs,

*pomeran@nucl-th.sinp.msu.ru
†rubtsova@nucl-th.sinp.msu.ru
‡kulikov@nucl-th.sinp.msu.ru

only the discretized spectra of the above Hamiltonians are required.

In this paper, we take a step much further and consider multichannel problems, in particular, the two-body coupled-channels problem and the three-body problem including long-range Coulomb interactions. As a particular L^2 representation, we consider the multichannel Gaussian basis, which is very convenient for few-body bound-state calculations [24]. We also employ an additional procedure for combining spectra found using bases with slightly changed parameters into a common set with the same integrated density [19,20] without increasing the basis dimension.

The structure of the article is as follows. In Sec. II, we define the main objects that will be used to solve multichannel problems. Here the spectral and integrated densities of states for the Hamilton matrix in a discrete basis are introduced. The formalism allows us to find phase shifts, as well as the density of continuum levels. In this section, we also present a technique for constructing a dense union of discretized spectra obtained using different Gaussian bases of the same dimension. Section III explains how to calculate the total integrated densities of states and resonance parameters in the multichannel two-body problem. The application of the above technique to the three-body problem and the results for light nuclei with $A = 6$ are considered in Sec. IV. A summary is provided in the last section. For the reader's convenience, we add an Appendix with a brief description of the three-body spectral functions given in Ref. [23].

II. SPECTRAL DENSITIES FOR A DISCRETIZED CONTINUUM

Below, up to Sec. IV, we consider a two-body system with a single-channel or multichannel interaction operator V. It is assumed that this interaction, which relates the asymptotic Hamiltonian H_0 and the total (perturbed) Hamiltonian H,

$$H = H_0 + V, \tag{1}$$

satisfies the standard conditions of the scattering problem [25]. In particular, it is assumed that the operators H and H_0 are Hermitian, their continuous spectra coincide, and the operator V has a finite trace.

A. Continuum level density and the spectral shift function

In our treatment, we use two basic functions, the spectral shift function $\xi(E)$ and the continuum level density $\Delta(E)$. Both them are related to the S-matrix as follows:

$$\xi(E) = -\frac{1}{2\pi i}\ln\det S(E), \tag{2}$$

$$\Delta(E) = -\frac{d\xi}{dE} = \frac{1}{2\pi i}\mathrm{Tr}\left[S(E)^{\dagger}\frac{dS(E)}{dE}\right]. \tag{3}$$

Equation (2) is known in the scattering theory as the Birman-Krein formula [22]. It is important to emphasize that Eq. (2) is not a definition of the SSF $\xi(E)$; this function is determined independently using the trace formula or the Fredholm determinant. The existence of the spectral shift function ξ and the validity of Eq. (2) are proved, in particular, for the interaction operators V with a finite trace. Similarly, Eq. (3) is not a conventional definition for the continuum level density, which is usually introduced as a trace of the difference between the imaginary parts of the total and asymptotic resolvents [10,23] (see also Appendix) or as the difference of the spectral densities for the total and asymptotic Hamiltonians (see details in, e.g., Ref. [19]). However, for our purposes, the above relations (2) and (3) are most convenient.

The functions $\xi(E)$ and $\Delta(E)$ are expressed in terms of the eigen phase shifts and their derivatives respectively:

$$\xi(E) = -\frac{1}{\pi}\sum_{\nu=1}^{K}\delta_\nu(E), \quad \Delta(E) = \frac{1}{\pi}\sum_{\nu=1}^{K}\frac{d\delta_\nu(E)}{dE}, \tag{4}$$

where K is the number of the opened channels at energy E and $\delta_\nu(E)$ are the eigen phase shifts for the multichannel S matrix.

The presence of a resonance pole in the S matrix, which is close to the real energy axis, manifests itself in the on-shell energy dependence of all its elements. Therefore, for the energy region near the resonance position, the functions $\xi(E)$ and $\Delta(E)$ can be parametrized as follows [7,10]:

$$\xi(E) = -\frac{1}{\pi}\arctan\left(\frac{E-E_R}{\Gamma/2}\right) + \xi_{\mathrm{bg}}(E), \tag{5}$$

$$\Delta(E) = \frac{1}{\pi}\frac{\Gamma/2}{(E-E_R)^2+\Gamma^2/4} + \Delta_{\mathrm{bg}}(E), \tag{6}$$

where E_R and Γ are the position and the width of the resonance, respectively, $\xi_{bg}(E)$ and $\Delta_{bg}(E)$ are the background functions, which change slowly near the resonance compared to the resonance terms. Thus, both functions $\xi(E)$ and $\Delta(E)$ exhibit a specific behavior and each of them could be used to find the resonance parameters.

B. Spectral densities for a discretized continuum

In the previous paper [19], we developed the formalism for an approximate evaluation of $\xi(E)$ and $\Delta(E)$ functions in a single-channel scattering via the L^2 continuum discretization.

In this approach, both Hamiltonians H and H_0 are represented by finite matrices in some basis constructed from L^2 functions. Therefore the corresponding spectra are pure discrete and consist of finite number of eigenvalues. In such a case, one can introduce individual ISDs $X(E)$ and $X_0(E)$ for the total H and asymptotic H_0 Hamiltonians, correspondingly.

Each of the functions $X(E)$ and $X_0(E)$ is determined by the number of eigenvalues of the corresponding matrix Hamiltonian that are less than or equal to the energy E. Thus, by a definition, the functions $X(E)$ and $X_0(E)$ for discretized spectra are integer step functions whose values increase by 1 for each value of E equal to the eigenvalue of the corresponding Hamiltonian. However, we can assume that there are smooth monotonic functions $X(E)$ and $X_0(E)$, whose values for $E = E_j$ coincide with the corresponding integer values. The value of such a function at all other points $E \neq E_j$ can be determined by using an interpolation.

In fact, $X(E)$ is an inverse function for the function $E(j)$, which determines the dependence of the eigenvalue on its ordinal number j. Therefore, $X(E)$ depends on the method of the continuum discretization, i.e., on the type and parameters

of the basis functions and on the basis dimension (see details and examples in Ref. [19]).

Using the reconstructed continuous functions $X(E)$ and $X_0(E)$, one can approximate the spectral shift function ξ in terms of their difference [19]:

$$\xi(E) = X_0(E) - X(E). \tag{7}$$

Having the continuous integrated spectral densities $X(E)$ and $X_0(E)$, one can also determine the individual spectral densities of the discretized continuum for the total and asymptotic Hamiltonians,

$$\rho(E) = \frac{dX(E)}{dE}, \quad \rho_0(E) = \frac{dX_0(E)}{dE}, \tag{8}$$

and the continuum level density as their difference:

$$\Delta(E) = \rho(E) - \rho_0(E). \tag{9}$$

Let us consider the question of the convergence of results when expanding the basis. When calculating bound states, their energies obtained from a diagonalization of the Hamiltonian matrix converge to exact values when the dimension of the basis N tends to infinity. In contrast, each eigenvalue of a discretized continuous spectrum tends to the continuum threshold. Moreover, continuous functions $X_0(E)$, $X(E)$ and $\rho(E)$, $\rho_0(E)$, representing individual integrated and spectral densities for each of the operators H and H_0, do not have finite limits at $N \to \infty$ [19]. It should be emphasized that the spectral density of a truly continuous spectrum of some Hamiltonian cannot be determined at all.

However, the corresponding differences (7) and (9) under certain conditions converge to the exact functions $\xi(E)$ and $\Delta(E)$ when the dimension of the basis N increases [19]. We can define a small parameter $\alpha \sim 1/N$, which determines the convergence and allows us to estimate an error for the function $\xi(E)$, i.e., for the scattering phase shift (see Ref. [19] for details).

Thus, the integrated spectral density $X(E)$ recovered from the discretized spectrum of the matrix Hamiltonian is the key object of our approach. Below we will show how to practically construct such a density for a multichannel problem and even for a three-body problem.

C. Union of the discretized spectra

In the present calculations, we use the set of the Gaussian basis functions

$$\phi_{ilm}(\mathbf{r}) = \varphi_l(\beta_i, r) Y_l^m(\hat{\mathbf{r}}), \quad i = 1, \ldots, N, \tag{10}$$

$$\varphi_l(\beta, r) = A_{\beta,l} r^{l+1} \exp(-\beta r^2). \tag{11}$$

Here $A_{\beta,l}$ are normalization factors, Y_l^m are spherical functions, and β_i are Gaussian parameters defined by some function $g(x)$ as follows:

$$\beta_i = \beta_0 g\left(\frac{i}{N+1}\right), \quad i = 1, \ldots, N. \tag{12}$$

Under certain conditions on the function $g(x)$, the set of functions (10) forms a complete nonorthogonal basis at the limit $N \to \infty$, which we will refer to as the Gaussian basis. The function $g(x)$ must map the interval $(0, 1)$ into the interval $(0, \infty)$, be monotonic on the interval $(0, 1)$, and behave at zero as $g(u) \sim u^a$, $a \geqslant 1$. In our calculations, to define the set of Gaussian parameters $\{\beta_i\}$, we usually use the so-called generalized Chebyshev grid, which is specified by the function

$$g(x) = \left[\tan\left(\frac{\pi}{2}x\right)\right]^t \tag{13}$$

and, in our experience, provides the most economical Gaussian basis for bound state calculations [26].

It has been shown [at least for few particular functions $g(x)$ including (13)] that, by using a finite shift a of the index i in Eq. (12), one gets a transformation of the basis that does not change the eigenvalue distribution. Let us introduce a new (shifted) parameter set $\{\beta_i(a)\}$ as follows:

$$\beta_i(a) = \beta_0 g\left(\frac{i-a}{N+1}\right), \quad i = 1, \ldots, N, \tag{14}$$

where $0 \leqslant a < 1$. As a result of the diagonalization of the Hamiltonian matrix on the new basis with the parameter set (14), we obtain a new shifted set of eigenvalues that lie on the same curve $E(x)$:

$$E_i(a) = E(i-a). \tag{15}$$

This property of invariance of the discretized spectrum allows to combine several spectra into one common spectral set. To do this, we use the following procedure. Consider M sets of parameters $\{\beta_i^m\}_{i=1}^N$, $m = 1, \ldots, M$ for the basis functions:

$$\left\{\beta_i^m = \beta_0 g\left(\frac{i-a_m}{N+1}\right)\right\}_{i=1}^N, \quad m = 1, \ldots, M, \tag{16}$$

where a_m is a sequence of the additional shift parameters $0 \leqslant a_1 < \cdots < a_m < \cdots < a_M < 1$.

Using sets (16), one gets M different Gaussian bases of the same dimension N, each of which results in a set of the eigenvalues $\{E_i^m\}_{i=1}^N$ after a diagonalization of the Hamiltonian matrix. All these eigenvalues are described by the same function $E(x)$ and the same ISD $X(E)$ according to Eq. (15), so that they are combined in the union of discretized spectra. This union results in an M-fold densification of the discretized continuum when the functions $E(x)$ and $X(E)$ are defined on a much denser set of points than the initial single diagonalization gives.

This union of spectra is illustrated in Fig. 1 where a uniform distribution of the additional shift parameters is used: $a_m = (m-1)/M$.

Based on the idea of the union of discretized spectra, we have developed a new technique for solving single-channel scattering problems (calculating the scattering phase shifts) and finding the resonance parameters [19].

It should be noted that for a single-channel problem (when the continuous spectrum is simple) one can study the behavior of each energy level E_j depending on the shift parameter a in a set of Gaussian parameters. Such an approach can be considered as an analog of the well-known stabilization method [27], where the decrease of the shift a is used instead of increasing the dimension of the basis [20].

However, in the multichannel case, and even more so in the few-body problem, when the continuous spectrum is not simple, the dependence of each eigenvalue on the shift parameters

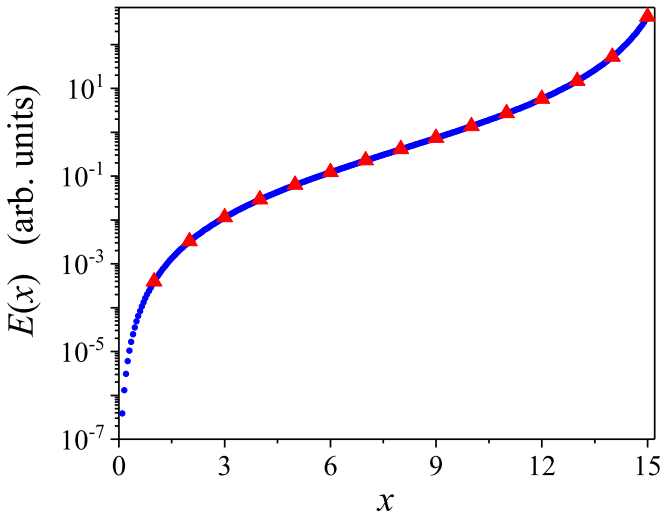

FIG. 1. The initial discretized spectrum (triangles) for the asymptotic Hamiltonian found in the Gaussian basis with the dimension $N = 15$ and the united spectral set (dots) with the multiplicity $M = 20$.

is not suitable for analysis. Below we will apply a statistical processing of the spectrum union which allows us to analyze the whole discretized spectrum regardless of the multiplicity of the original continuum.

III. MULTICHANNEL TWO-BODY PROBLEM

Consider a general multichannel problem with a matrix Hamiltonian:

$$H_{\mu\nu} = H_{0\nu}\delta_{\mu\nu} + V_{\mu\nu}, \quad \mu, \nu = 1, \ldots, K. \tag{17}$$

Here the multichannel asymptotic Hamiltonian has a diagonal form:

$$\mathbf{H}_0 = \mathrm{diag}[H_{01}, \ldots, H_{0\nu}, \ldots, H_{0K}], \tag{18}$$

where each channel asymptotic Hamiltonian $H_{0\nu}$ includes the kinetic energy operator, the possible Coulomb interaction, and the threshold energy E^{ν}_{th}.

For present calculations, we use the multichannel Gaussian basis as a combination of the single-channel bases (10):

$$\left\{\phi^{\nu}_{il_\nu m_\nu}(\mathbf{r}) = \varphi_{l_\nu}\left(\beta^{\nu}_i, r\right)Y^{m_\nu}_{l_\nu}(\hat{\mathbf{r}}),\ i = 1, \ldots, N^{\nu}\right\}^{K}_{\nu=1}, \tag{19}$$

where l_ν and m_ν are the orbital momentum in the channel ν and its projection correspondingly.

Because the matrix of the asymptotic Hamiltonian (18) is diagonal, the integrated density $X_0(E)$ is the sum of the integrated densities $X_{0\nu}(E)$ for each channel ν and can be easily calculated.

However, a construction of the integrated densities for the total Hamiltonian is an ambiguous task. Actually, the whole discretized spectrum should be divided into separate branches according to its multiplicity. In our previous papers [18,20], we have shown that such a separation can be performed in the case when the discretized spectrum of the multichannel asymptotic Hamiltonian is degenerate with the required multiplicity. Such degeneracy can be achieved using the basis of wave packets [18], as well as in some special cases, when all the thresholds are the same [20]. In the general case, this requirement is not satisfied.

Nevertheless, below we will show that such a division of the spectrum into separate branches is not necessary when it is needed to find only "cumulative" quantities, such as the sum of eigen phase shifts and the total continuum level density from Eq. (4) or the position and total width of a resonance.

A. Numerical reconstruction of the integrated density of states

One can try to recover the functions $X(E)$ and $\rho(E)$ directly using their definitions in terms of the number of eigenstates that are below or near the energy E, respectively. For example, let us divide the entire energy interval $[0, E_{\max}]$ into "pockets" ΔE_i and calculate the number of eigenvalues of the corresponding Hamiltonian ΔN_i inside each pocket. Then the approximations for the spectral and integrated densities are determined as follows:

$$\rho_i = \frac{\Delta N_i}{\Delta E_i}, \quad X_i = \sum_{j\leqslant i}\rho_j \Delta E_j = \sum_{j\leqslant i}\Delta N_j. \tag{20}$$

To find the function $\xi(E)$ one should calculate the difference between the integrated density $X(E)$ and the integrated density for the asymptotic multichannel Hamiltonian $X_0(E)$:

$$X_0(E) = \sum_{\nu=1}^{K} X_{0\nu}(E). \tag{21}$$

This difference approximately determines the sum of the eigen phase shifts:

$$\sum_{\nu=1}^{K_0}\delta_\nu(E) = \pi[X(E) - X_0(E)], \tag{22}$$

where K_0 is the number of the opened channels. Although in this way one gets only the sum of the eigen phase shifts, this is sufficient to determine the parameters of the resonance.

The union of the discretized spectra allows one to get a much more dense spectral set and treat the problem "statistically." In this case, the values from Eq. (20) should be additionally divided by the factor M (the number of spectra in the union):

$$\rho^U_i = \frac{\Delta N_i}{M\Delta E_i}, \quad X^U_i = \frac{1}{M}\sum_{j\leqslant i}\Delta N_j. \tag{23}$$

Below we use two types of such "statistical" processing of the spectrum: (a) when the energy width of the pocket ΔE_i is fixed and (b) when the number of the states ΔN_i in the pocket is fixed. If the functions $X(E)$ and $\rho(E)$ exist, both methods should give the same results.

As a visual example, Fig. 2 shows the spectral and integrated densities for the two-channel problem from Sec. III B, reconstructed by using the union of 100 discretized spectra with basis dimensions $N_1 = N_2 = 20$ and a rather wide pocket width $\Delta E = 0.5$ arb. units. In further calculations, we use a much smaller pocket width, which allows us to better simulate the continuous dependence on energy.

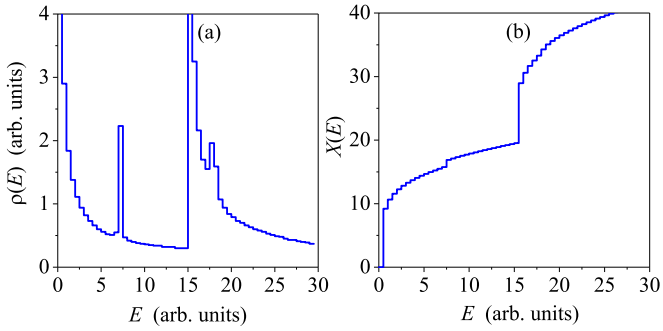

FIG. 2. The reconstructed spectral (a) and integrated (b) densities of the states for the two-channel problem with the shifted thresholds from Sec. III B.

It should be noted that the method of a reconstruction the functions $X(E)$ and $\rho(E)$ for a simple spectrum described in Sec. II is a special case of the procedure proposed here with $\Delta N_i = 1$ (the smallest pocket).

B. Two-channel problem with the shifted thresholds

Consider a model two-channel problem with the shifted thresholds. This example uses arbitrary units $\hbar = m = 1$ and we will omit all measurement units in the text of this subsection to simplify notations.

The asymptotic Hamiltonian is diagonal and has two components:

$$H_{01} = -\frac{1}{2}\frac{d^2}{dr^2}, \quad H_{02} = -\frac{1}{2}\frac{d^2}{dr^2} + E_{\rm th}, \tag{24}$$

where $E_{\rm th} = 15$ is the threshold energy for the second channel. The interaction is given by the matrix[1]

$$\mathbf{V}(r) = \begin{pmatrix} 15e^{-0.5r^2} & 5re^{-r^2} \\ 5re^{-r^2} & 15(2r^2 - r - 1)e^{-r^2} \end{pmatrix}. \tag{25}$$

1. Union of spectra for the two-channel problem

We consider first how the technique with the union of the discretized spectra works for the multichannel problem. Here again the variety of the basis sets are constructed using finite shifts of the arguments in the Gaussian parameters (14). The properties of the united spectra can be illustrated by the example of the multichannel asymptotic Hamiltonian $\mathbf{H}_0$. Here we have the "exact" integrated density X_0 equal to the sum of the densities of the individual channels $X_{0\nu}$, which are easily calculated. On the other hand, we can calculate statistically the same cumulative density X_0 according to Eq. (23) and compare it with the "exact" one.

Figure 3 shows the integrated density X_0 reconstructed by Eq. (23) from the union of the spectra found in the two-channel Gaussian bases defined on the Chebyshev grids (13) with $t = 3$ and dimensions $N_1 = N_2 = 20$ for the different multiplicities of union M and $\Delta N_i = 1$ in comparison with the sum of the individual integrated densities $X_{0\nu}$.

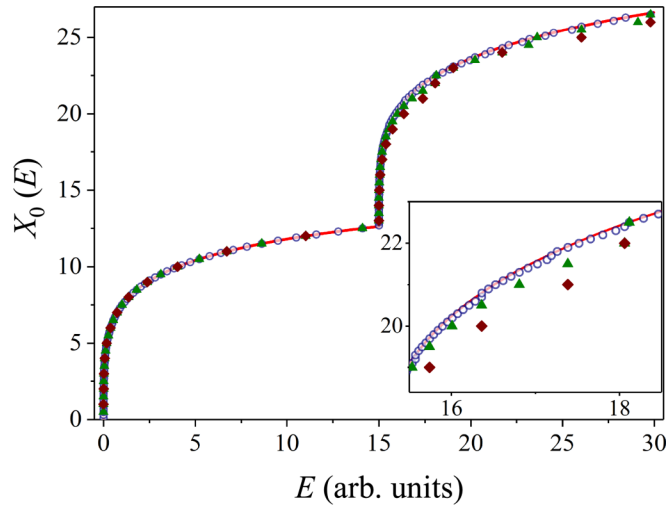

FIG. 3. The cumulative integrated density $X_0(E)$ for the two-channel problem with shifted thresholds found in the two-channel Gaussian bases with dimensions $N_1 = N_2 = 20$ for the different multiplicity of union: $M = 1$ (filled diamonds), $M = 2$ (filled triangles), $M = 10$ (empty circles). The solid curve shows the sum of ISDs for the separate channels $X_0^1(E) + X_0^2(E)$. The inset panel shows a small interval above the second threshold energy $E_{\rm th} = 15$ arb. units.

The case with $M = 1$ corresponds to the original spectrum found as a result of one diagonalization. It can be seen that the unions of spectra with the different multiplicities M lead to the same function $X_0(E)$ for $E < E_{\rm th}$, since the spectrum of the original problem is simple there. However, above $E_{\rm th}$, where the spectrum is doubly degenerate, the corresponding approximations differ for small M. At the same time, as the value of M increases, the corresponding function $X_0(E)$ approaches the exact sum (21).

Thus, employing the union of the discretized spectra in a multichannel problem provides more advantages. This allows us to obtain more accurate the cumulative ISD $X_0(E)$ for the multichannel Hamiltonian even in the case with the shifted thresholds.

2. Sum of the eigen phase shifts and the continuum level density

Figure 4 shows a comparison of the sum of the eigen phase shifts for the problem (24)-(25), found from the union of discretized spectra with the multiplicity $M = 160$ and from the direct solution of the corresponding coupled Schrödinger equations (the "exact" result). Here we use the two-channel Gaussian basis with dimensions $N_1 + N_2$, constructed using the Chebyshev grid (13) with $t = 2.6$ and $\beta_0 = 1$ for both channels. To process the discretized spectra, a procedure with fixed energy pockets $\Delta E = 0.1$ was applied. The result obtained from a continuum discretization with a basis dimension $N_1 = N_2 = 30$ is nearly indistinguishable from the "exact" one.

There are two resonances for the model problem in question. The resonance parameters are found from the fitting by the Breit-Wigner form (6) of the differences of the spectral

[1]The form of the potential is taken from Ref. [15]. However, we use here the Gaussians instead of the exponential functions.

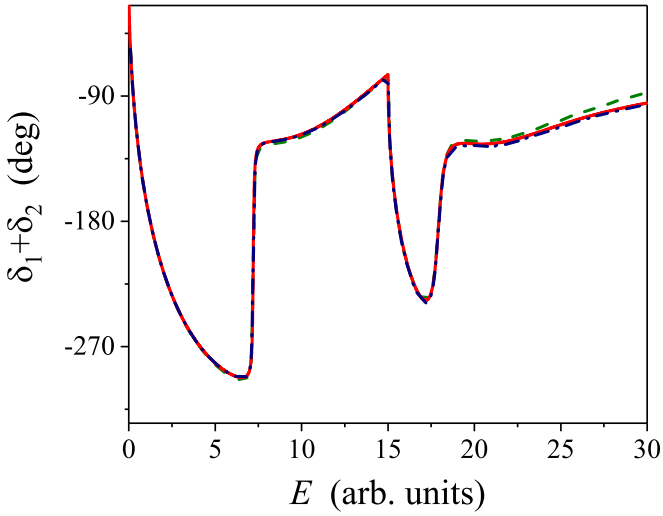

FIG. 4. The sum of the eigen phase shifts for the model problem with the interaction (25) found from the discretized spectra in the Gaussian bases of dimensions $N_1 = N_2 = 22$ (dashed curve) and $N_1 = N_2 = 30$ (dash-dotted curve) with the multiplicity $M = 160$. The result of a direct solution of the coupled-channels Schrödinger equations is shown by the solid curve.

functions $\rho(E)$ and $\rho_0(E)$ which are reconstructed from the union of the discretized spectra. The first resonance is situated below the threshold of the second channel. Therefore, the spectrum in this region is simple, and a relatively small densification with $M = 20$ is sufficient to find the resonance parameters. Here the spectral densities $\rho(E)$ and $\rho_0(E)$ can be determined from Eq. (23) with $\Delta N_i = 1$, i.e., as numerical derivatives of the integrated densities (calculated from two points). The corresponding continuum level density $\rho(E) - \rho_0(E)$ and the fitting function are represented in Fig. 5.

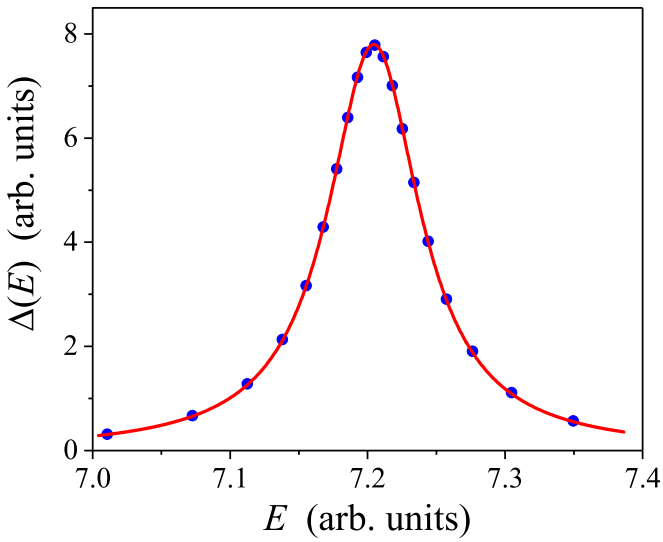

FIG. 5. The continuum level density for the two-channel model (25) near the first resonance state position found from the discretized spectra using the Gaussian basis with $N_1 = N_2 = 30$ and $M = 20$ (dots) and the fitting function (solid curve).

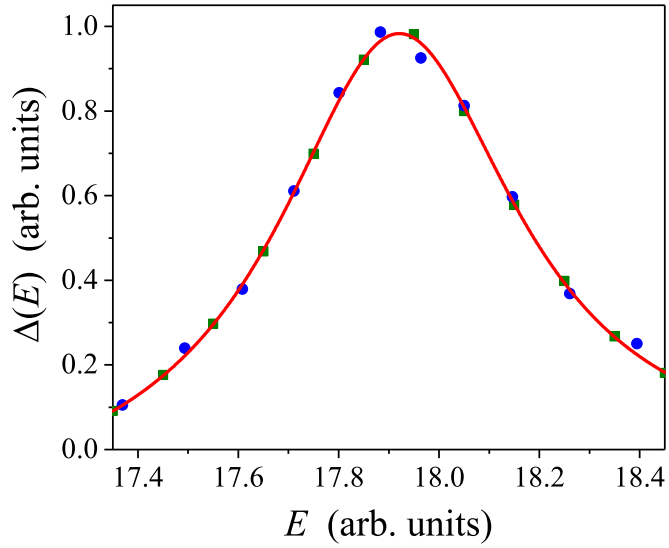

FIG. 6. The continuum level density for the two-channel model (25) near the second resonance state position found employing the 200-fold union of the Gaussian spectra with the basis dimensions $N_1 = N_2 = 30$ and two types of pockets: With the fixed energy $\Delta E_i = 0.1$ (squares) and with the fixed number of states $\Delta N_i = 30$ (circles). The fitting function is shown by a solid curve.

The resonance parameters found from this fit, $E_R = 7.204(1)$ and $\Gamma = 0.0814(7)$, agree with the values extracted from a solution of the Schrödinger equation, $E_R = 7.205$ and $\Gamma = 0.0820$. Here the errors in the parentheses are given by the fitting procedure.

The second resonance is above the threshold energy $E_{\text{th}} = 15$. Therefore, to obtain a smooth approximation for the spectral density, one needs to use the union of the discretized spectra with a much higher multiplicity M up to 200.

The corresponding approximations for $\Delta(E)$ found by using the methods (a) and (b), i.e., with the pockets defined by fixed energy steps and the pockets containing a fixed number of the states, in comparison with the fitting function, are presented in Fig. 6. Here both methods give nearly the same continuum level density and the obtained resonance parameters are the following: $E_R = 17.919(5)$ and $\Gamma = 0.584(8)$ (the corresponding values found from the solution of the Schrödinger equation are $E_R = 17.92$ and $\Gamma = 0.596$). The errors of the found parameters is estimated from the fitting procedure for $\Delta E_i = 0.075$.

3. Resonance parameters from the integrated density

It is also possible to extract the resonance parameters from the approximation of the integrated density $X(E)$ in a form:

$$X(E) = \frac{1}{\pi} \arctan\left(\frac{E - E_R}{\Gamma/2}\right) + X_{\text{bg}}(E), \tag{26}$$

which follows from Eq. (5). Here it is assumed that the background function $X_{\text{bg}}(E)$ includes the integrated density $X_0(E)$ corresponding to the asymptotic Hamiltonian and, therefore, does not contain a resonance term. Thus, the background

TABLE I. The parameters of the resonance E_R and Γ (in arb.units) found by fitting the functions $X(E)$ and $X(E) - X_0(E)$ for $N_1 = N_2 = 22$ and different M.

	$X(E)$		$X(E) - X_0(E)$	
M	E_R	Γ	E_R	Γ
20	17.92(4)	0.59(5)	17.94(6)	0.58(7)
40	17.92(2)	0.60(2)	17.93(2)	0.58(2)
80	17.920(6)	0.596(6)	17.918(7)	0.591(8)
160	17.919(2)	0.594(2)	17.919(3)	0.589(3)

function in the resonance region can be approximated by a polynomial of a small degree.

This method seems simpler and more convenient for calculations since there is no need in a calculation of the integrated density for the asymptotic Hamiltonian, and it does not require a good approximation for the derivative dX/dE using Eq. (23). Therefore, one may use pockets with $\Delta N_i = 1$ here. On the other hand, more parameters may be needed to get a good approximation for the background function in Eq. (26).

The convergence of the results of fitting both function $X(E)$ and the difference $X(E) - X_0(E)$ with increasing multiplicity of the union M are presented in Table I. Here, the second-degree polynomials were used to approximate the background functions in both cases.

The values in the parentheses in Table I are the absolute errors given by the fitting procedure. It is clear that these errors are decreasing with increasing M. At the same time, the 20-fold densification already gives a reasonable approximation.

The convergence of the parameters with increasing the basis dimension for $M = 160$ is shown in Fig. 7. Here the uncertainties again correspond to the fitting procedure.

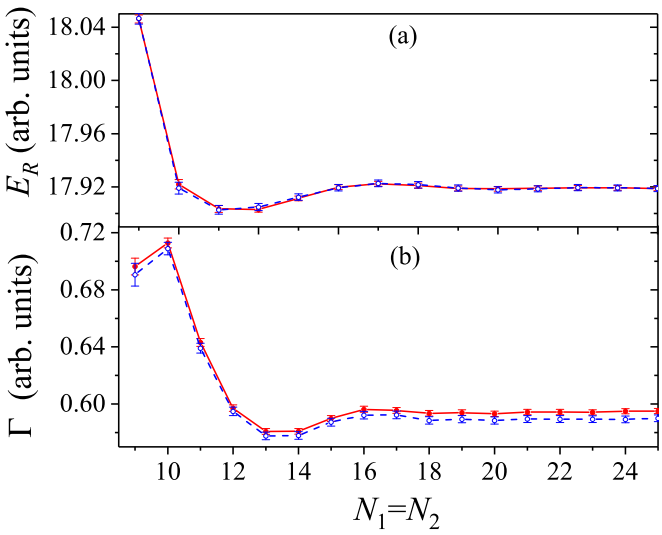

FIG. 7. The values of the resonance position E_R (a) and width Γ (b) for the two-channel model (25) found from fitting the functions $X(E)$ (solid curve with filled circles) and $X(E) - X_0(E)$ (dash-dotted curve with empty circles) for the different basis dimensions $N_1 = N_2$.

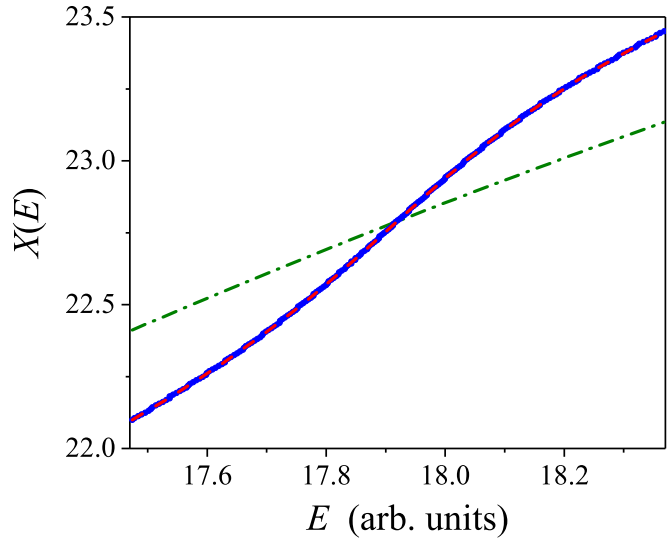

FIG. 8. The ISD $X(E)$ for the two-channel model (25) found using the Gaussian basis (dots) with $N = 22$ and $M = 160$ near the second resonance position, the fitting function (solid curve), and the background function (dash-dotted curve).

Both calculations give the same result for the resonance position $E_R = 17.919(2)$. The value of the width found from fitting the function $X(E)$ is $\Gamma = 0.595(2)$, while fitting of the difference $X(E) - X_0(E)$ results in the value $\Gamma = 0.590(2)$. In all cases, the absolute errors are given from treating the results for the basis dimensions $N_1 = N_2$ in the range 18–25. The light difference in the values of the width may be caused by an approximation of the background function $X_{\rm bg}(E)$. At the same time, one can conclude that the resonance parameters can be found rather accurately just from the function $X(E)$, which should be useful for the three-body problems.

Figure 8 shows the IDS $X(E)$ for the two-channel model (25) found using the Gaussian basis, the fitting function (26), and the background function $X_{\rm bg}(E)$. The approximation for $X(E)$ is very good.

C. Two-channel problem with a tensor coupling

As a second numerical example, consider the NN scattering problem for the coupled ${}^3S_1 - {}^3D_1$ channels in the framework of a hybrid model that takes into account non-nucleonic degrees of freedom. In the simplest version of the model, these non-nucleonic degrees of freedom are described by an internal six-quark channel that includes one bound state. For this calculation, we slightly modified the model from Ref. [28], eliminating the possibility of describing inelastic processes. The Hamiltonian of the modified model has the form

$$\mathbf{H} = \mathbf{H}_0 + \mathbf{V}, \quad \mathbf{H}_0 = \mathrm{diag}[T_S, T_D, E_0|\alpha\rangle\langle\alpha|],$$
$$\mathbf{V} = \begin{pmatrix} V_{SS}^{\rm ext} & V_{SD}^{\rm ext} & \mu_S|\varphi_S\rangle\langle\alpha| \\ V_{DS}^{\rm ext} & V_{DD}^{\rm ext} & \mu_D|\varphi_D\rangle\langle\alpha| \\ \mu_S|\alpha\rangle\langle\varphi_S| & \mu_D|\alpha\rangle\langle\varphi_D| & 0 \end{pmatrix}. \quad (27)$$

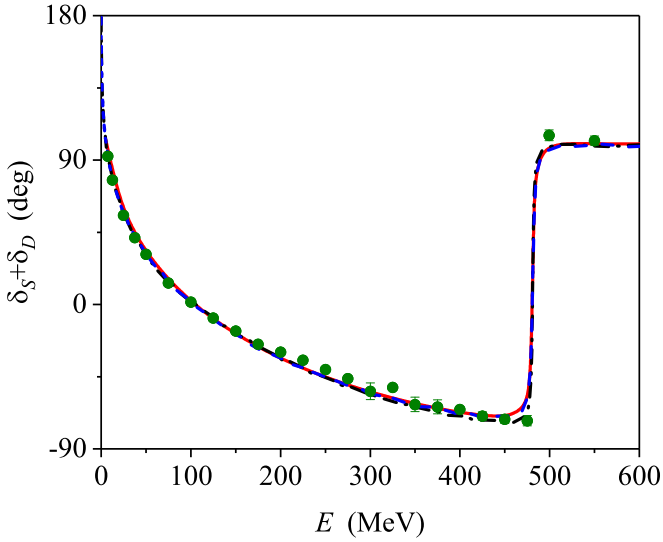

FIG. 9. The sum of the eigen phase shifts for the coupled ${}^3S_1 - {}^3D_1$ channels found using 80 Gaussian bases of dimensions $N_1 = N_2 = 10$ (black dash-dotted curve) and $N_1 = N_2 = 30$ (blue dashed curve) in comparison with the result found from a solution of the coupled Lippmann-Schwinger equations (red solid curve) and the SAID data (see the text). Solid and dashed curves are nearly indistinguishable in the figure.

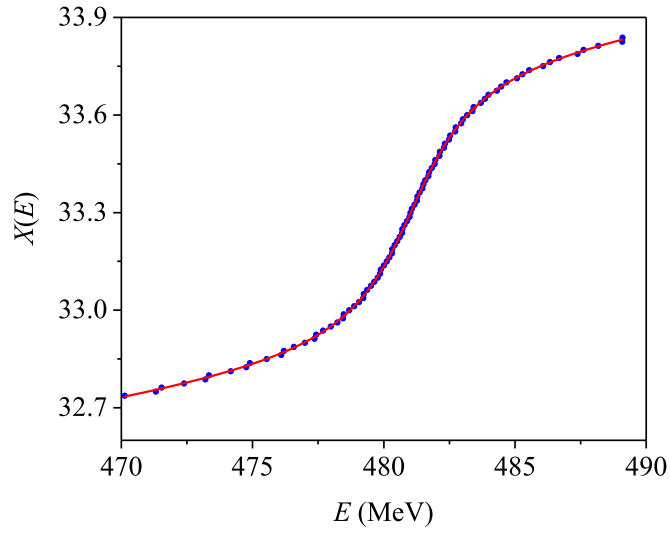

FIG. 10. The function $X(E)$ found using the Gaussian bases of dimensions $N_1 = N_2 = 30$ with the union multiplicity $M = 80$ (dots) in comparison with the fitting function (solid curve).

Here T_S and T_D are the kinetic energy operators for S and D waves, V^{ext} is the NN interaction in the external channel, and $\mu_{S(D)}$ and $|\varphi_{S(D)}\rangle$ are the coupling constants and form factors for the transition operator between the NN and internal channels. The external interaction V^{ext} includes the one-pion exchange potential and the orthogonalizing nonlocal potential which provides the required repulsion between nucleons. The detailed description of the model and its parameters can be found in Ref. [28]. The energy of the state $|\alpha\rangle$ in the internal channel is $E_0 = 440$ MeV.

Formally, this problem is a three-channel one. However, the asymptotic Hamiltonian of the internal channel does not have a continuous spectrum, so the scattering process is possible only in two external (S- and D-wave) channels. At the same time, due to coupling with the internal channel, there exists a resonance state corresponding to the total Hamiltonian near the energy E_0.

The sum of the eigen phase shifts found from the discretized spectra is shown in Fig. 9. For a comparison, we also present in the figure the sum of the ${}^3S_1$ and ${}^3D_1$ partial phase shifts found from a numerical solution of the coupled-channels Lippmann-Schwinger equations for the above model and from the SAID partial wave analysis[2] [29]. The last two points from the SAID results are shifted up by 180°. Here, one can conclude that even the use of the basis of the relatively small dimensions $N_1 = N_2 = 10$ results in a good approximation for the sum of the eigen phase shifts in a wide energy region. The parameters of the resonance can be found from fitting of the function $X(E)$ with the function (26). The result of such fitting is shown in Fig. 10, where the dots represent $X(E)$ found using the Gaussian bases with dimensions $N_1 = N_2 = 30$ and $M = 80$. The parameters of the resonance are the following: $E_R = 481.1$ MeV and $\Gamma = 3.85$ MeV. These values are very close to the results extracted from solving the coupled Lippmann-Schwinger equations: $E_R = 480.9$ MeV and $\Gamma = 3.61$ MeV.[3]

IV. THREE-BODY PROBLEM

The continuous spectrum of the three-body Hamiltonian is infinite-fold degenerate. Therefore, the analysis of the discretized spectrum obtained from the diagonalization of the Hamiltonian matrix on the basis of L^2 functions turns out to be much more complicated compared to the case of the multichannel problem. Here it is impossible to divide the discretized spectrum into separate branches and determine the S matrix. Nevertheless, densifying the spectrum set by the union of the discretized spectra makes it possible in many cases to find a position and a total width of the three-body resonance. We will demonstrate the applicability of such an approach using the three-cluster $\alpha + 2N$ model for the six-nucleon nuclei as an example.

A. Spectral densities for the three-body problem

The spectral shift function formalism on which our approach is based in the two-body case cannot be directly generalized to the three-body problem. In the two-body scattering problem (single- or multichannel), one deals with two operators—the total and asymptotic Hamiltonians—and their

[2]Here the solutions at single energies are taken and the represented energy corresponds to the half of the laboratory energy given in the SAID data.

[3]Because we have modified the interaction these resonance parameters differ from those found in Ref. [28].

difference is the perturbation that determines the scattering. The scattering problem for a three-body system is generally defined by five Hamiltonians: The total Hamiltonian H, three channel Hamiltonians H_i, each of which includes the interaction of only one pair of particles, and the three-body free Hamiltonian H_0 (the kinetic energy operator). The differences between the total and any of four of the above asymptotic Hamiltonians, in contrast to the two-body problem, are not operators with a finite trace. However, this does not mean that spectral densities could not be defined here.

In Ref. [23], the authors shows that one can define the spectral function $\Omega_+(E)$ for the third virial coefficient, which is related to the trace of the difference of the resolvents for the above five Hamiltonians (A7). The main result of the work [23] is the direct relation between the function $\Omega_+(E)$ and the three-body S matrix (for details, see the Appendix). Therefore, we can expect that, in the presence of a resonance, the function $\Omega_+(E)$ contains the Breit-Wigner term.

As the result of the continuum discretization procedure, one has finite matrices of the operators. So, as in the two-body case the individual spectral densities might be constructed for the discretized spectra of all five Hamiltonians. Using the analogy with the difference of individual spectral densities (9), one can write the three-body spectral function $\Delta_3(E) \equiv \Omega_+(E)/\pi$ as follows [see Eq. (A11)]:

$$\Delta_3(E) = \rho(E) - \rho_0(E) - \sum_{i=1}^{3} [\rho_i(E) - \rho_0(E)], \qquad (28)$$

where $\rho(E)$, $\rho_i(E)$ $(i = 0, 1, 2, 3)$ are the individual spectral densities related to the Hamiltonians H and $H_i (i = 0, 1, 2, 3)$ respectively.

Each of these densities does not exist for the original continuous spectrum, but their difference, at least in the form (28), should have a limit as the basis dimension increases. Thus, the formalism [23] gives some mathematical justification for the analysis of spectral densities in the three-body case.

It should be noted that the above discussion is applicable only in the case without the long-range Coulomb interactions. When the long-range Coulomb interactions are included the problem becomes much more complicated from the mathematical point of view. Below we will assume that in the L^2 representation one can consider finite matrices and construct spectral densities for the case with charged particles as well. But the question of the existence of the limit of the differences, e.g., in the form (28), remains open here.

One can take a further step and construct the integrated spectral densities for each Hamiltonian similarly to the two-body case. It should be emphasized that the resonance behavior should manifest itself only in the integrated spectral density $X(E)$ of the total Hamiltonian H, because the possible resonances refer to H only. Therefore, we expect that $X(E)$ can be approximated by the same Eq. (26), but the background function here should have a more complicated form.

In the examples considered below, we use the differences between the spectral and integrated densities for the total Hamiltonian and only one of the asymptotic Hamiltonians. These density differences do not correspond to any spectral functions for a true continuum above the three-body decay threshold. However, the analysis of such differences makes it possible to reduce the effect of background functions when fitting the resonance term.

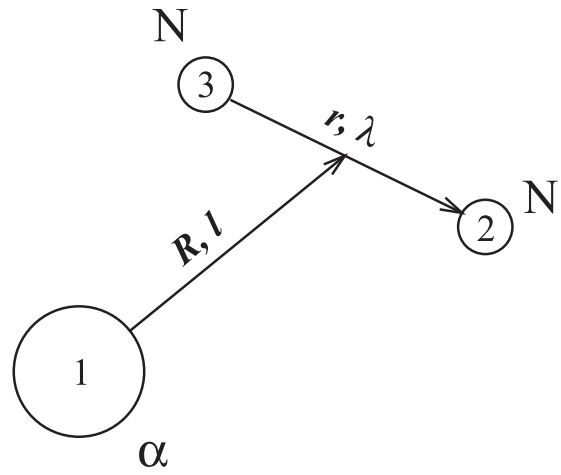

FIG. 11. Jacobi coordinates **r** and **R** and respective angular momenta **λ** and ***l*** for the $\alpha + 2N$ system.

Below we check the above assumptions on the example of the three-cluster $\alpha + 2N$ model for the six-nucleon nuclei.

B. Three-cluster model for the αNN system and the basis

The three-cluster model was successfully used in the1980s and 1990s to describe the lowest states of nuclei ^{6}He, ^{6}Li, and ^{6}Be [30–32]. Here we use the version of the three-cluster model from [31] defined by the Hamiltonian

$$H^3 = T + V_{N_2\alpha} + V_{N_3\alpha} + V_{NN}. \qquad (29)$$

Here T is the kinetic energy, $V_{N_i\alpha}$ is the potential of the interaction of the ith nucleon with the α particle (the quasilocal potential with the even-odd splitting and with the forbidden $0S$ state is used), and V_{NN} is the Reid soft core NN potential. In the case when one or both nucleons are protons, the required long-range Coulomb interactions are included into potentials. The explicit form and parameters of the potentials are given in [31]. In this paper, we use the above model just as an example of a three-body system for finding resonance parameters and, therefore, do not discuss its physical validity and its advantages and disadvantages. We only note that the version [31] gives some underbinding of the ground states of the nuclei ^{6}He and ^{6}Li.

The notation for the Jacobi coordinates and the orbital angular momenta for the $\alpha + 2N$ system is shown in Fig. 11: **r** is the relative coordinate of two nucleons, while **R** is the Jacobi coordinate of the α particle relative to the center of mass of the nucleon pair, and the orbital angular momenta λ and l correspond to the Jacobi coordinates **r** and **R**, respectively.

The three-body system wave function $\Psi^{JM_J}(\mathbf{r}, \mathbf{R})$ with the total angular momentum J and its projection M_J is expanded in a series of the basis functions Φ^{γ}_{ij}:

$$\Psi^{JM_J}(\mathbf{r}, \mathbf{R}) = \sum_{\gamma} \sum_{i=1}^{N_r} \sum_{j=1}^{N_R} C^{\gamma}_{ij} \Phi^{\gamma}_{ij}(\mathbf{r}, \mathbf{R}), \qquad (30)$$

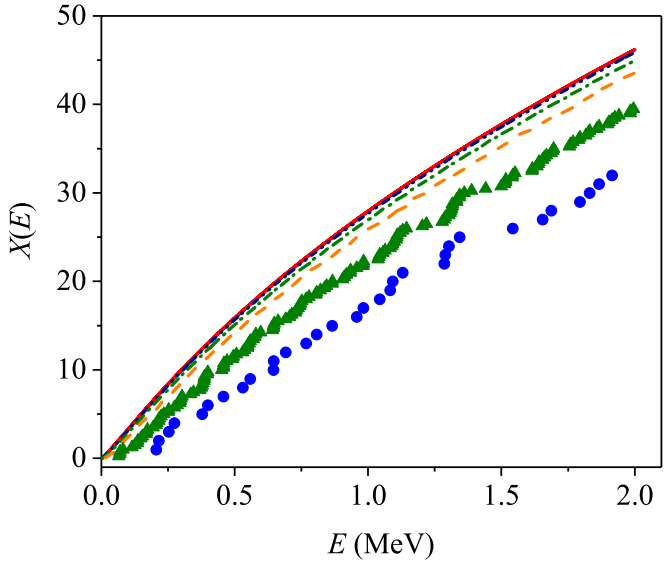

FIG. 12. The integrated spectral density for the αpp asymptotic Hamiltonian found with different unions: $M_r = M_R = 1$ (filled circles), $M_r = M_R = 2$ (filled triangles), $M_r = M_R = 5$ (dashed curve), $M_r = M_R = 10$ (dash-dotted curve), $M_r = M_R = 25$ (dash-dot-dotted curve), and $M_r = M_R = 50$ (solid curve).

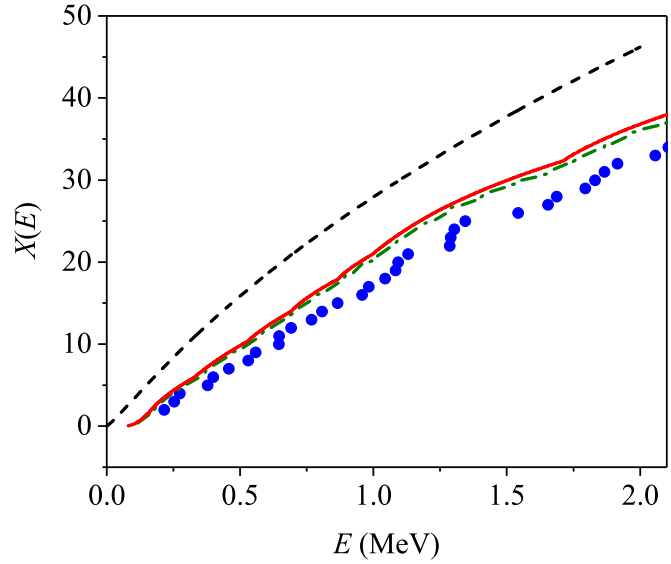

FIG. 13. The integrated spectral density for the αpp asymptotic Hamiltonian found with different values of M_R and $M_r = 1$: $M_R = 1$ (filled circles), $M_R = 5$ (dash-dotted curve), and $M_R = 50$ (solid curve). The integrated density for $M_r = M_R = 50$ is shown as the dashed curve.

where C_{ij}^{γ} are the unknown coefficients and the composite index $\gamma = \{\lambda, l, L, S\}$ is the set of quantum numbers of the basis function: λ, l, $\boldsymbol{L} = \boldsymbol{l} + \boldsymbol{\lambda}$, and S is the total spin of two nucleons.

The six-dimensional basis functions Φ_{ij}^{γ} are constructed from the product of the Gaussian functions (11) and the spin-angular factors $W_{\gamma}^{JM_J}$:

$$\Phi_{ij}^{\gamma}(\mathbf{r}, \mathbf{R}) = \varphi_{\lambda}\left(\alpha_i^{\gamma}, r\right)\varphi_l\left(\beta_j^{\gamma}, R\right)W_{\gamma}^{JM_J}(\hat{\mathbf{r}}, \hat{\mathbf{R}}), \quad (31)$$

$$W_{\gamma}^{JM_J}(\hat{\mathbf{r}}, \hat{\mathbf{R}}) = \{[Y_{\lambda}(\hat{\mathbf{r}}) \times Y_l(\hat{\mathbf{R}})]_L \times [\chi_{1/2}(N_2) \times \chi_{1/2}(N_3)]_S\}_{JM_J}, \quad (32)$$

where $\chi_{1/2}(N_i)$ is the spin function of the ith nucleon. The total isospin I is equal to the isospin of the pair of nucleons and is therefore uniquely determined by the values of λ and S.

C. Union of discretized spectra in the three-body problem

To construct the union of spectra in the three-body case, one has more opportunities than in the two-body problem. In particular, the basis functions from Eq. (31) have two independent sets of the parameters α_i^{γ} and β_j^{γ}, and for each of them one can employ the procedure with a shift of the index given by Eq. (14). So, one can introduce two set of shifts $\{a_m^r\}_{m=1}^{M_r}$ and $\{a_m^R\}_{m=1}^{M_R}$. Then the full number of bases employed to construct the union is equal to $M = M_r \times M_R$. Combining all M spectra obtained using these bases, one can try to construct the spectral density and integrated density using Eq. (23). The result of such a union is shown in Fig. 12, where the integrated densities $X(E)$ calculated with different values of M for the asymptotic αpp Hamiltonian for the $J^P I = 0^+1$ state are shown. The asymptotic Hamiltonian includes the kinetic energy operator and three Coulomb interactions between three charged particles. Here we use the three-body Gaussian basis with four partial components [see Eq. (35)] and the symmetric union of the spectra when $M_r = M_R$.

As one can see from Fig. 12, with increasing the union multiplicity M, the integrated density $X(E)$ converges. However, the convergence result depends on the union method. In Fig. 13, we compare the above "converged" result for $X(E)$ with the results corresponding the union of the spectra obtained by changing only the R dependence of basis functions, i.e., with $M_r = 1$.

Here the "converged" integrated density $X_{M_r=1}(E)$ (shown by the solid curve) differs from the result for the symmetric ($M_r = M_R$) densification (shown by the dashed curve). Also one can see that the curve $X_{M_r=1}(E)$ consists of several smooth segments. In fact, such an integrated density corresponds to the coupled-channels reduction of the initial three-body spectrum. With such a reduction, the continuous three-body spectrum is replaced by a multichannel spectrum with nonphysical thresholds determined by the discretized spectrum of the pp subsystem. Such an approximation can also be used for practical calculations, but numerical solutions may have additional singularities due to the presence of these nonphysical thresholds [33].

Thus, in the three-body problem, densifying the spectrum set involving a variation of the basis parameters over both variables allows one to decrease nonphysical effects caused by a continuum discretization.

D. The state 3^+0 of nucleus ^{6}Li and D_3 phase shift in α-d scattering

The three-cluster $\alpha + n + p$ model, which describes the lowest states of the ^{6}Li nucleus with isospin $I = 0$, gives an example of a three-particle system in which there is a

TABLE II. The quantum numbers and the dimensions of the basis components for a calculation of the 3^+0 state of ^{6}Li.

$\gamma = \lambda lLS$	$N_r \times N_\rho$
0221	15 × 20
2021	15 × 20
2221	15 × 20
2231	15 × 20
2241	15 × 20
2421	8 × 8
4221	8 × 8
4041	8 × 8

bound state (deuteron) of one pair of particles (nucleons). The continuous spectrum of this system starts from $E_d = -2.224$ MeV and up to the three-particle breakup threshold $E = 0$ is doubly degenerate, like the spectrum of the two-channel problem.

The first excited state $J^P I = 3^+0$ of the ^{6}Li nucleus with an energy -1.514 MeV is below the three-particle threshold and has a width of 24 keV. This state is actually a two-particle α-d resonance (the contribution of the noncluster components does not exceed 1%) and manifests itself in the D_3 phase shift of the α-d scattering. Although the continuous spectrum at $E < 0$ is doubly degenerate due to the coupling of the channels D_3 and G_3, the contribution of the states with $\lambda = 4$ at $E < 0$ is very small ($\approx$0.5%). Therefore, this coupling can be neglected and the spectrum in this region can be considered as simple.

In the region of the simple spectrum, one can calculate the phase shifts and the resonance parameters from the difference of the integrated densities $X(E)$ and $X_0(E)$ for the total and asymptotic Hamiltonians in accordance with Eq. (7), which was used to analyze the discretized spectra of the two-body systems [19]. The asymptotic Hamiltonian includes the total kinetic energy T, the np interaction, and the Coulomb interaction between the proton and the α particle:

$$H^3_{\rm asy} = T + V^{\rm Coul}_{p\alpha} + V_{np}. \tag{33}$$

The spectra of the Hamiltonians H^3 and $H^3_{\rm asy}$ were calculated using the Gaussian basis with the parameters α_i, β_j specified on the Chebyshev grid (13) with $t = 2.6$. The basis includes eight spin-orbit configurations (channels), the quantum numbers and the corresponding dimensions of which are listed in Table II. The ground state of lithium 1^+0 in the model [31] has an underbinding by 0.43 MeV. To get a more realistic description of the resonance, we increased the $N\alpha$ interaction coupling constants by 2.1% so that the calculated binding energy of the ^{6}Li ground state 1^+0 matches the experimental value.

To reconstruct the functions $X(E)$ and $X_0(E)$ on a dense set of points, we used the union of M_R spectra obtained by changing the Gaussian parameters β_j of the basis functions $\varphi_l(\beta_j, R)$ by the index shift. The resulting D_3 phase shift of the α-d scattering is shown in Fig. 14. The phase shift analysis data are also presented in this figure.

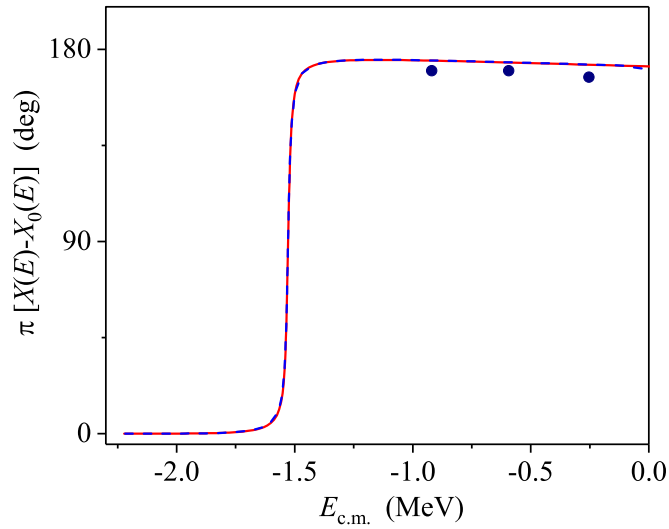

FIG. 14. The D_3 phase shift of the α-d scattering found from the difference of the integrated spectral densities $X(E)$ and $X_0(E)$ for the $\alpha + 2N$ model by using the union with $M_R = 10$ (dashed curve) and $M_R = 30$ (solid curve). Dots show the phase shift analysis data [34].

The energy derivative of the above D_3 phase shift is shown in Fig. 15. Fitting of this dependence according to the Breit-Wigner form results in the following values for the ^{6}Li(3^+0) resonance parameters:

$$E_R = -1.528 \text{ MeV}, \quad \Gamma = 22 \text{ keV}, \tag{34}$$

which are in a reasonable agreement with the experimental values -1.514 MeV and 24 keV, respectively.

It should be noted that, although in this case the continuous spectrum in the region $E < 0$ can be considered as simple, the existence of the spectral shift function $\xi(E)$ related to

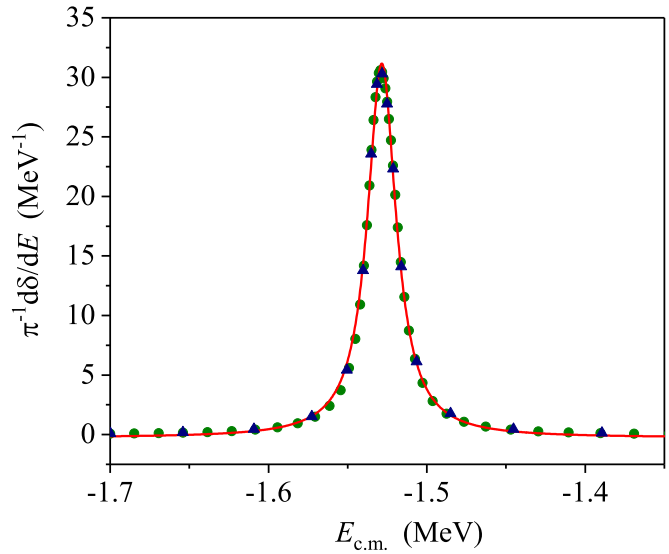

FIG. 15. The numerical derivative of the D_3 phase shift of the α-d scattering found from the union with $M_R = 10$ (triangles) and $M_R = 30$ (circles). The solid curve shows the Breit-Wigner parametrization.

the S matrix by the Birman-Krein formula (2) has not been mathematically proved. As already mentioned, in contrast to the multichannel problem, the perturbation in the three-body scattering problem, i.e., the difference of the operators H^3 and $H^3_{\rm asy}$, does not have a finite trace. Nevertheless, the above results show that the method of calculating the phase shift through the difference in the integrated densities of the discretized spectra works in the region of the simple spectrum for the three-body problem as well.

E. Ground state of ^{6}Be (0^+1)

The ground state of the nucleus ^{6}Be (0^+1) is unstable. Its experimental energy is equal to 1.371 MeV relative to the α-p-p threshold and its width is equal to 92 keV. One of the most detailed theoretical studies for this state within the three-body approach is presented in Ref. [2] based on solving coupled equations in a hyperspherical representation.

Treatment of the isovector states within the framework of the three-cluster model gives an example of a three-body system without pairwise bound states, where the infinitely degenerated continuous spectrum starts from the three-body breakup threshold $E = 0$. Therefore, in the calculations, a symmetric densifying of the spectrum set is used. In particular, the union of $M = M_r \times M_R$ spectra is constructed by changing basis parameters corresponding to both variables r and R.

The calculations are performed with taking into account four spin-orbit basis configurations with the quantum numbers

$$\gamma = \{\lambda, l, L, S\} = \{0000\},\ \{1111\},\ \{2200\},\ \{3311\}, \quad (35)$$

with the same dimensions $N = N_r \times N_\rho$, $N_r = N_\rho$, so that the total basis dimension is equal $N = 4 \times N_r^2$. The $N\alpha$ interaction was increased by ≈3% so that the calculated position of the resonance E_R would nearly match the experimental value.

Here, as the asymptotic Hamiltonian we use the following one with switched off nuclear part of the interaction:

$$H^3_{\rm asy} = T + V^{\rm Coul}_{p_1\alpha} + V^{\rm Coul}_{p_2\alpha} + V^{\rm Coul}_{p_1p_2}, \quad (36)$$

where p_1 and p_2 denote protons.

Figure 16 shows the integrated densities $X_0(E)$ and $X(E)$ for the asymptotic and total Hamiltonians, respectively, for the system α-p-p (0^+1), which are obtained from $M = 9000$ diagonalizations (the symmetric densification in r and R) on the above four-component basis. The presence of a resonance at $E \approx 1.38$ MeV can be seen from the behavior of the total integrated density $X(E)$.

The difference of the integrated densities for the total and asymptotic Hamiltonians multiplied by π is shown in Fig. 17. It should be emphasized that this difference no longer corresponds to any phase shift. However it demonstrates characteristic resonance behavior near the assumed resonance energy which is quite similar to that seen in the two-body case.

Therefore, below we approximate both the individual function $X(E)$ and the difference $X(E) - X_0(E)$ in accordance with Eqs. (26) and (5). The results of such fitting in the resonance region $1.25 < E < 1.5$ MeV are presented in Table III, as well as in Fig. 18. The errors indicated in the parentheses are related to the fitting procedure itself.

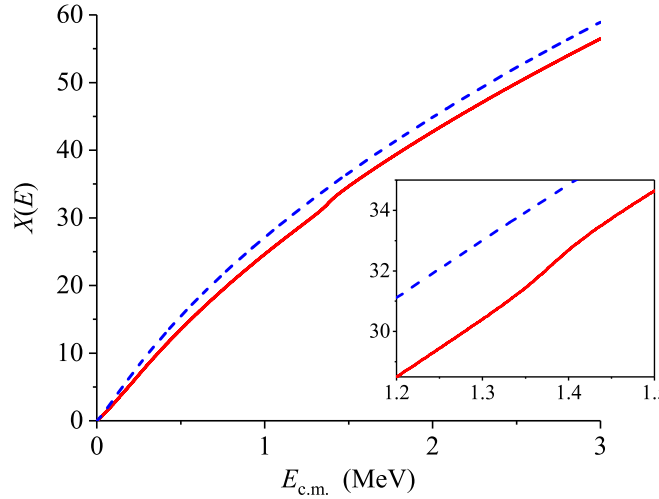

FIG. 16. The integrated densities $X(E)$ and $X_0(E)$ for the asymptotic and total Hamiltonians of the system α-p-p (0^+1) found in the Gaussian bases from Eq. (35) by using the symmetric union with $M_r \times M_R = 30 \times 30$. The inset shows a small energy interval near the resonance position.

From Fig. 18 it is clear that the values of E_R and Γ have some deviations from their average values when the dimension of the basis changes in the region where convergence has already been achieved. This scatter is taken into account when assessing the final errors of the results. In particular, the parameter values are found by averaging the results for N_r from 16 to 20, and the corresponding mean absolute errors are taken.

Finally, both calculations [with $X(E)$ and with the difference $X(E) - X0(E)$] give fairly close results for the resonance parameters. The data with estimated errors are the

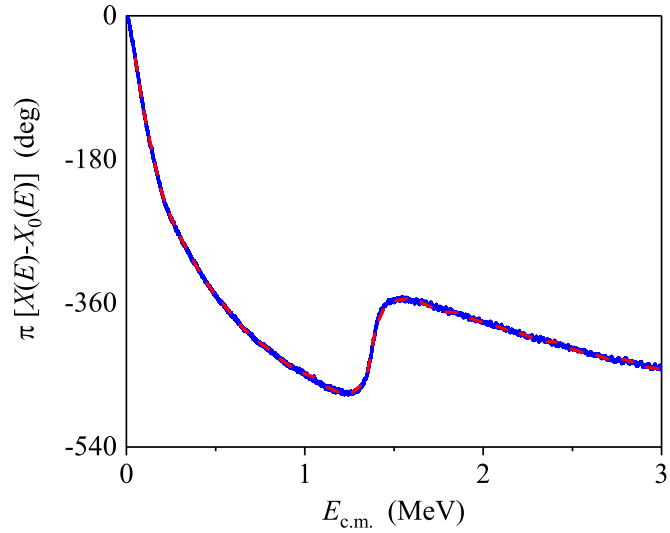

FIG. 17. The difference of integrated densities $X(E) - X_0(E)$ for the asymptotic and total Hamiltonians of the system α-p-p (0^+1) found in the Gaussian bases by using the union of the $M_r \times M_R = 30 \times 30$ spectra. Solid blue curve: Calculation with fixed $\Delta N_i = 1$; dashed red curve: Calculation with fixed $\Delta E_i = 0.05$ MeV.

TABLE III. The energies and widths of the ground state ^{6}Be (in MeV) found using the Gaussian bases with different dimensions $N_r \times N_R$ and $M = 30 \times 30$ by fitting the functions $X(E)$ and $X(E) - X_0(E)$.

	$X(E)$		$X(E) - X_0(E)$	
$N_r = N_R$	E_R	Γ	E_R	Γ
9	1.262(1)	0.144(1)	1.259(1)	0.146(1)
10	1.261(1)	0.111(1)	1.258(1)	0.111(1)
11	1.41356(7)	0.0800(2)	1.41364(8)	0.0802(3)
12	1.39698(8)	0.0799(1)	1.39682(9)	0.0796(2)
13	1.38911(7)	0.0819(1)	1.38893(7)	0.0812(1)
14	1.38274(7)	0.0781(1)	1.38273(9)	0.0777(1)
15	1.38132(6)	0.0796(1)	1.38138(9)	0.0795(1)
16	1.38088(6)	0.0798(1)	1.38074(8)	0.0800(1)
17	1.37773(6)	0.0795(1)	1.37786(8)	0.0791(1)
18	1.37951(6)	0.0794(1)	1.37940(8)	0.0793(1)
19	1.37807(7)	0.0801(1)	1.37819(8)	0.0799(1)
20	1.37865(7)	0.0807(1)	1.37827(9)	0.0805(1)

following:

$$E_R = 1.379 \pm 0.001 \text{ MeV}, \quad \Gamma = 79.8 \pm 0.5 \text{ keV}, \quad (37)$$

which are in reasonable agreement with the experimental values.

Figure 19 shows the quality of the fit of the function $X(E)$ for the maximal basis dimension $N_r = N_R = 20$ in the resonance region and the background function $X_{\text{bg}}(E)$. The fitting function is indistinguishable from the numerically reconstructed $X(E)$.

Alternatively, having dense spectral sets, it is possible to reconstruct the three-body analog for the continuum level density $\Delta(E)$ as the difference between the spectral densities

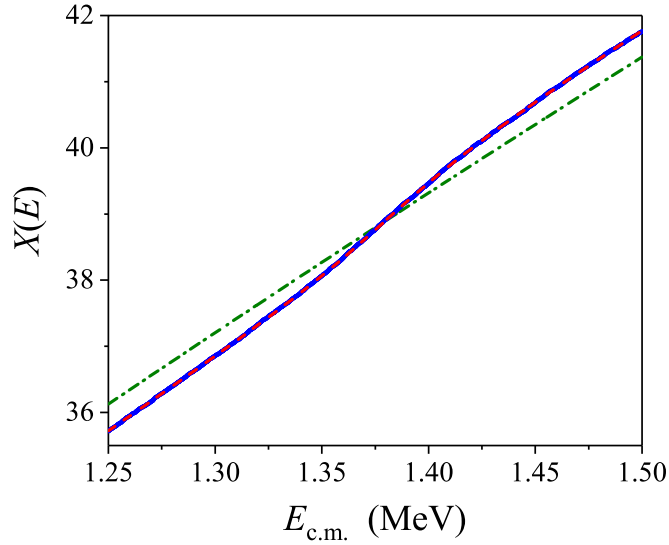

FIG. 19. The integrated density $X(E)$ for ^{6}Be(0^+1) in the resonance region found in the Gaussian bases with dimensions $N_r = N_R = 20$ by using the union of $M = 30 \times 30$ spectra (blue dots), the fitting function (red dashed curve), and the background function $X_{\text{bg}}(E)$ (green dash-dotted curve).

$\rho(E)$ and $\rho_0(E)$. In contrast with the two-body case this difference has no finite limit with increasing basis dimension. However, the corresponding subtraction allows one to decrease the influence of the background. Figure 20 shows such a function in the resonance region calculated using pockets of the same energy width of $\Delta E_i = 0.02$ MeV. The Breit–Wigner parametrization of such a density results in close values of the resonance parameters: $E_R = 1.378(1)$ MeV, $\Gamma = 81(3)$ keV. Here the errors are given by the fitting procedure. It can be

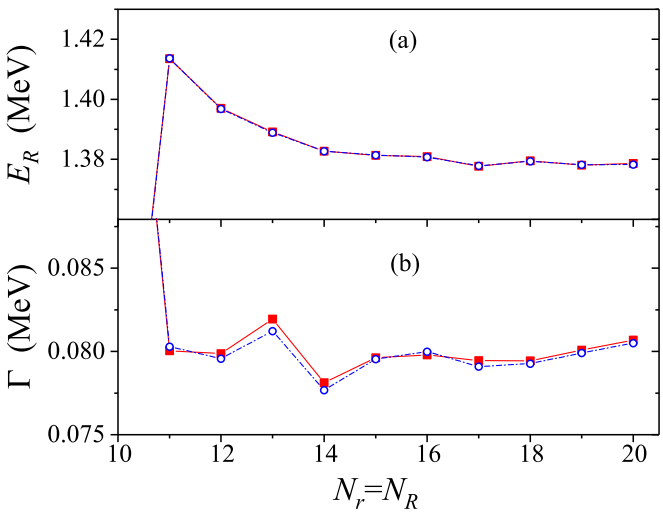

FIG. 18. The values of the resonance positions E_R (a) and widths Γ (b) for the the system α-p-p(0^+1) found from fitting the functions $X(E)$ (solid curve with filled squares) and $X(E) - X_0(E)$ (dash-dotted curve with empty circles) for different basis dimensions $N_r = N_R$.

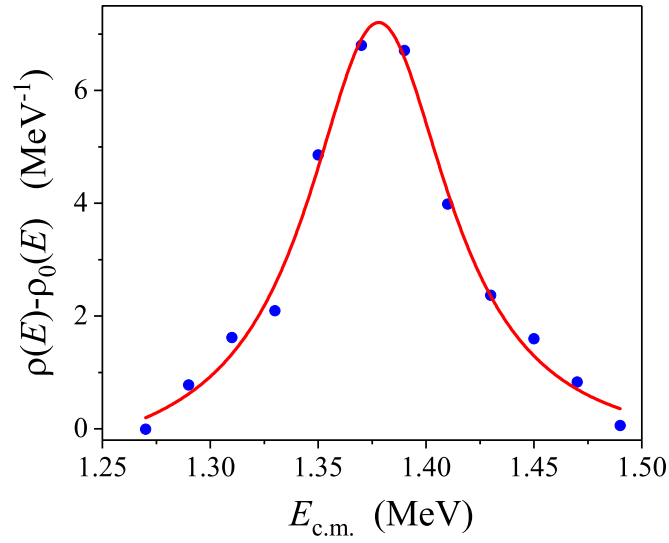

FIG. 20. The difference of the spectral densities $\rho(E) - \rho_0(E)$ for the α-p-p(0^+1) system near the resonance position found in the Gaussian bases with dimensions $N_r = N_R = 18$ by using the union of the 30×30 spectra (dots) and its fit by the Breit-Wigner form (solid curve).

concluded that the uncertainties in the results when fitting the X functions are smaller than those for fitting the difference of the spectral densities ρ.

Thus, having a sufficiently dense ordered set of the eigenvalues, which is a union of many discretized spectra of the matrix Hamiltonian, obtained on different Gaussian bases of the same dimensions, we were able to find the position and width of the three-particle resonance corresponding to the ^{6}Be(0^+1) state quite reliably. Three methods can be used for this purpose: a parametrization of the integrated density $X(E)$ for the total Hamiltonian, a parametrization of the difference of the integrated densities $X(E) - X_0(E)$ for the total and asymptotic Hamiltonians, and the Breit-Wigner parametrization of the difference of the spectral densities $\rho(E) - \rho_0(E)$. All three methods give close (within the margins of error) results. However, a parametrization of only one total integrated density $X(E)$ seems to be more preferable, since it does not require additional calculations with the asymptotic Hamiltonian and auxiliary interpolation procedures for the processing of spectral sets.

V. CONCLUSION

In this paper, we have introduced a new technique for finding the parameters of the resonances in multichannel and three-body systems from discretized continuous spectra. The method is based on two ideas: (i) recovering the spectral and integrated densities of the states and (ii) combining many discretized spectra with the same dimension, which allows one to get a much denser set of energy values covering the original continuous spectrum.

To determine the cumulative (total) decay width in the proposed approach, there is no need to consider in detail various types of boundary conditions. This width can be found directly from the analysis of the total discretized spectrum without dividing it into separate branches corresponding to different asymptotic channels. This simplifies drastically the practical solution of the problem. Also one can simultaneously consider the binary and three-body decay modes. Consequently, one can use only the Gaussian basis related to the binary channels to solve the problem rather than introducing additionally the hyperspherical basis to study a three-body decay mode.

Similarly to the complex scaling method, in the suggested approach one employs the same numerical scheme as for the bound states, i.e., a solution of the generalized eigenvalue problem for the Hamiltonian matrix; however, there is no need to use complex energies or momenta. In particular, to find the resonance parameters in the three-body case, one can use the same Gaussian basis of a rather moderate dimension as for calculating bound states. It is very important that the proposed approach avoids difficulties associated with the long-range Coulomb interactions and nonlocal interactions. This opens up the possibility of solving problems with three charged particles, such as two-proton radioactivity, using realistic models of the nucleon-nucleus interactions. We demonstrated the effectiveness of the method by calculating the width of the ^{6}Be ground state.

It should be emphasized that the proposed approach is applicable not only to the particular case considered here when the discretized spectra obtained in the Gaussian basis are used for analysis. The formalism based on the spectral and integrated densities of states can also be useful in other approaches employing the L^2 discretization of the continuum. In particular, a rather similar approach was introduced in chemical physics [7] in the framework of finite volume calculations.

In our future studies, we plan to consider in more detail questions related to the accurate definition of the spectral function $\Omega(z)$ for the general three-body problem and the meaning of the individual integrated densities of states there. This may also open up the possibility of treating the three-body scattering problems.

ACKNOWLEDGMENT

The authors appreciate financial support from the Russian Science Foundation (RSF), Grant No. 23-22-00072. The authors thank Prof. Yu. M. Tchuvil'sky for very valuable discussions.

APPENDIX: SPECTRAL FUNCTION FOR A THREE-BODY PROBLEM

In Ref. [23], the authors considered the second and third virial coefficients and the spectral expansions for them. The spectral expansion for the second virial coefficient is related to the following spectral function:

$$\omega(z) = \mathrm{Tr}[\mathrm{Im}G(z) - \mathrm{Im}G_0(z)], \tag{A1}$$

where $G(z) = [H - z]^{-1}$ and $G_0(z) = [H_0 - z]^{-1}$ are the resolvents[4] for the total and asymptotic two-body Hamiltonians respectively, and z is a complex energy. The imaginary parts of the above operators are defined by the relation

$$\mathrm{Im}G(z) = \frac{1}{2i}[G(z) - G(z^*)]. \tag{A2}$$

It can be shown that at real energies the function ω is just proportional to the continuum level density (3) (see, e.g., [10]):

$$\omega_+(E) = \pi\Delta(E), \quad \omega_+(E) \equiv \lim_{\epsilon\to 0}\omega(E + i\epsilon). \tag{A3}$$

It is related to the two-body S-matrix by the equation [23]

$$\omega_+(E) = \frac{1}{2i}\mathrm{Tr}\left[S(E)^\dagger\frac{dS(E)}{dE}\right]. \tag{A4}$$

Note that in the energy discretized representation the individual spectral densities $\rho(E)$ and $\rho_0(E)$ for the total and asymptotic Hamiltonians can be defined. So, one can write the following relation [10]:

$$\frac{1}{\pi}\mathrm{Tr}[\mathrm{Im}G(E + i0) - \mathrm{Im}G_0(E + i0)] = \rho(E) - \rho_0(E). \tag{A5}$$

[4]Here we use the same definition for a resolvent as in Ref. [23].

This results in Eq. (9) for the continuum level density and the function ω:

$$\omega_+(E) = \pi\Delta(E) = \pi[\rho(E) - \rho_0(E)]. \tag{A6}$$

For the three-body problem and the third virial coefficient, one can define [23] the spectral function via a more complicated difference operator:

$$\Omega(z) = \mathrm{Tr}\,\mathrm{Im}G_C(z), \quad \Omega_+(E) \equiv \lim_{\epsilon\to 0}\Omega(E + i\epsilon). \tag{A7}$$

Here the operator difference is introduced:

$$G_C(z) = G(z) - G_0(z) - \sum_{i=1}^{3}[G_i(z) - G_0(z)], \tag{A8}$$

where $G(z) \equiv [H - z]^{-1}$ and $G_i(z) \equiv [H_i - z]^{-1} (i = 0, 1, 2, 3)$ are the resolvents of five Hamiltonians: The total Hamiltonian H and four asymptotic Hamiltonians $H_i (i = 0, 1, 2, 3)$. The imaginary part of G_C in Eq. (A7) is defined similarly to Eq. (A2). The important property of the operator $\mathrm{Im}\, G_C(z)$ is that its trace is finite.

The spectral function (A7) is related directly to the three-body S matrix but in a more complicated way:

$$\Omega_+(E) = \frac{1}{2i}\mathrm{Tr}\left[\left(S^\dagger\frac{\partial S}{\partial E}\right)_C - A(E)\right] + \frac{1}{2i}\mathrm{Tr}\bar{A}(E), \tag{A9}$$

where the following difference is introduced which includes the total S matrix and matrices S_i corresponding to three asymptotic (channel) Hamiltonians H_i:

$$\left(S^\dagger\frac{\partial S}{\partial E}\right)_C \equiv S^\dagger\frac{\partial S}{\partial E} - \sum_{i=1}^{3} S_i^\dagger\frac{\partial S_i}{\partial E}, \tag{A10}$$

and $A(E)$ and $\bar{A}(E)$ are the specific operators related to the channel Hamiltonians as well.

In the energy discretized representation, the individual spectral densities for each of five Hamiltonians can be defined. Similarly to Eqs. (A5) and (A6), one can write the following equation for the spectral function:

$$\Omega_+(E) = \pi\left[\rho(E) - \rho_0(E) - \sum_{i=1}^{3}[\rho_i(E) - \rho_0(E)]\right]. \tag{A11}$$

[1] L. Zhou, S.-M. Wang, D.-Q. Fang, and Y.-G. Ma, Nucl. Sci. Tech. **33**, 105 (2022).
[2] L. V. Grigorenko *et al.*, Phys. Rev. C **80**, 034602 (2009).
[3] V. I. Kukulin, V. M. Krasnopolsky, and J. Horácek, *Theory of Resonances: Principles and Applications*, Reidel Texts in the Mathematical Sciences (Springer, Amsterdam, 1989).
[4] R. Lazauskas, Few-Body Syst. **64**, 24 (2023).
[5] P. Descouvemont and D. Baye, Rep. Prog. Phys. **73**, 036301 (2010).
[6] A. M. Shirokov, G. Papadimitriou, A. I. Mazur, I. A. Mazur, R. Roth, and J. P. Vary, Phys. Rev. Lett. **117**, 182502 (2016).
[7] V. A. Mandelshtam, T. R. Ravuri, and H. S. Taylor, J. Chem. Phys. **101**, 8792 (1994).
[8] S. Dietz, H.-W. Hammer, S. König, and A. Schwenk, Phys. Rev. C **105**, 064002 (2022).
[9] J. Casal and J. Gómez-Camacho, Phys. Rev. C **99**, 014604 (2019).
[10] K. Arai and A. T. Kruppa, Phys. Rev. C **60**, 064315 (1999).
[11] A. Csótó, Phys. Rev. C **49**, 3035 (1994).
[12] N. Moiseyev, Phys. Rep. **302**, 212 (1998).
[13] S.-I. Ohtsubo, Y. Fukushima, M. Kamimura, and E. Hiyama, Progr. Theor. Exp. Phys. **2013**, 073D02 (2013).
[14] S. M. Wang, N. Michel, W. Nazarewicz, and F. R. Xu, Phys. Rev. C **96**, 044307 (2017).
[15] G. V. Sitnikov and O. I. Tolstikhin, Phys. Rev. A **67**, 032714 (2003).
[16] M. Gómez-Rocha and E. R. Arriola, Phys. Lett. B **800**, 135107 (2020).
[17] C. W. Johnson *et al.*, J. Phys. G: Nucl. Part. Phys. **47**, 123001 (2020).
[18] O. A. Rubtsova, V. I. Kukulin, V. N. Pomerantsev, and A. Faessler, Phys. Rev. C **81**, 064003 (2010).
[19] O. A. Rubtsova and V. N. Pomerantsev, J. Phys. A **55**, 095301 (2022).
[20] V. N. Pomerantsev and O. A. Rubtsova, Phys. At. Nucl. **85**, 1087 (2022).
[21] D. R. Yafaev, *Mathematical Scattering Theory. General Theory* (AMS, Providence, RI, 1992).
[22] M. S. Birman and M. G. Krein, Dokl. Akad. Nauk SSSR **144**, 475 (1962) [Sov. Math. Dokl. **3**, 740 (1962)].
[23] V. S. Buslaev and S. P. Merkuriev, Theor. Math. Phys. **5**, 1216 (1970).
[24] E. Hiyama, Y. Kino, and M. Kamimura, Prog. Part. Nucl. Phys. **51**, 223 (2003).
[25] R. G. Newton, *Scattering Theory of Waves and Particles* (McGraw-Hill, New York, 1966).
[26] V. I. Kukulin, V. M. Krasnopolsky, V. T. Voronchev, and P. B. Sazonov, Nucl. Phys. A **453**, 365 (1986).
[27] A. U. Hazi and H. S. Taylor, Phys. Rev. A **1**, 1109 (1970).
[28] V. I. Kukulin, V. N. Pomerantsev, O. A. Rubtsova, M. N. Platonova, and I. T. Obukhovsky, Chin. Phys. C **46**, 114106 (2022).
[29] R. L. Workman, W. J. Briscoe, and I. I. Strakovsky, Phys. Rev. C **94**, 065203 (2016); all SAID PWA solutions can be accessed via the website, http://gwdac.phys.gwu.edu.
[30] V. T. Voronchev, V. M. Krasnopolsky, and V. I. Kukulin, J. Phys. G **8**, 649 (1982); V. T. Voronchev, V. M. Krasnopolsky, and V. I. Kukulin, and P. B. Sazonov, *ibid.* **8**, 667 (1982).
[31] V. I. Kukulin, V. N. Pomerantsev, Kh. D. Razikov, V. T. Voronchev, and G. G. Ryzhikh, Nucl. Phys. A **586**, 151 (1995).
[32] B. V. Danilin, M. V. Zhukov, S. N. Ershov, F. A. Gareev, R. S. Kurmanov, J. S. Vaagen, and J. M. Bang, Phys. Rev. C **43**, 2835 (1991).
[33] O. A. Rubtsova, V. I. Kukulin, and V. N. Pomerantsev, Phys. Rev. C **84**, 044002 (2011).
[34] P. A. Schmelzbach, W. Grüebler, V. König, and P. Marmier, Nucl. Phys. A **184**, 193 (1972).